

Tuning the hydrogenation activity of Pd NPs on Al-MIL-53 by linker modification†

Cite this: DOI: 10.1039/c3cy00910f

Damin Zhang,^a Yejun Guan,^{*a} Emiel J. M. Hensen,^b Teng Xue^a and Yimeng Wang^aReceived 11th November 2013,
Accepted 18th December 2013

DOI: 10.1039/c3cy00910f

www.rsc.org/catalysis

The hydrogenation activity of 3 wt% Pd nanoparticles supported on various mono-group (H, OCH₃, NH₂, Cl, and NO₂) substituted Al-MIL-53 materials has been investigated. Substituents enhanced the dispersion of palladium nanoparticles on Al-MIL-53, leading to a narrow particle size distribution in the range of 2 to 4 nm. Pd nanoparticles on fresh catalysts were present as a mixture of Pd(II) and Pd(0) with different ratios. These Pd species readily became metallic in a hydrogen flow even at room temperature. Their activities in hydrogenation of phenol and phenylacetylene are linked to the substituents on the aromatic ring of the framework. Catalysts with electron-donating groups (OCH₃ and NH₂) show much higher activity than those containing electron-withdrawing groups (Cl and NO₂). This behavior might be explained by the hydrogen dissociation abilities of metallic Pd nanoparticles affected by the organic linkers.

Introduction

Palladium-based catalysis plays a vital role in fine chemical production.^{1,2} One of the predominant applications of palladium catalysts is selective hydrogenation of unsaturated compounds, *e.g.*, phenol hydrogenation to cyclohexanone and semi-hydrogenation of alkynes.^{3–5} Cyclohexanone is of great industrial interest for the production of caprolactam and adipic acid.¹ Recent studies have suggested that very high activity can be achieved in liquid phase phenol hydrogenation at a relatively low temperature giving economic and efficiency advantages.^{4,5} This also opens the possibility to produce bio-adipic acid from lignin-derived biomass through hydrogenation of pyrolysis oil.⁶ Materials such as carbon nitride,⁷ polyaniline-functionalized carbon-nanotubes,⁸ ionic liquid-like copolymers,⁹ and metal organic frameworks (MOFs)^{10,11} have been reported to show improved hydrogenation activity for Pd compared to the use of conventional carrier materials. It is generally believed that an important ability of these novel supports is to affect the electronic properties of Pd nanoparticles.

Metal organic frameworks (MOFs) comprise networks of metal centers or inorganic clusters bridged by simple organic

linkers through metal–ligand coordination bonds. The possibility to use MOFs as supports for metal nanoparticles has already been studied in quite some detail.^{12,13} Compared with conventional porous inorganic materials such as zeolites, MOFs may display strong host–guest interactions between the framework and metal nanoparticles *via* coordination and π – π forces. These kinds of interactions have been proposed to enhance catalytic properties of supported catalysts for hydrogenation of ethyl cinnamate¹⁴ and alkenes,¹⁵ cross-coupling reactions,¹⁶ aerobic oxidation of alcohols,¹⁷ and especially hydrogenation of phenols¹⁰ and α -ketoesters.¹⁸ The introduction of various organic substituents in MOFs has been argued to change their electronic properties, a main effect being the modification of the electron density in the phenyl moieties of the organic linker by use of electron-withdrawing or -donating groups.¹⁹ For instance, introducing electron-withdrawing groups (*e.g.*, NO₂) in the organic linker of UiO-66 strongly enhances the Lewis acidity of coordinated Zr sites.²⁰ We surmise that such modifications in the electronic structure of the MOF may also affect the properties of Pd nanoparticles dispersed on their surface.

To date, there has been no report on the effect of organic linkers whose electronic properties are modified through substituents on the catalytic properties of MOF-supported noble metal nanoparticles. In this study, a series of mono-substituted Al-MIL-53 have been synthesized using a one-step hydrothermal method using substituted terephthalic acid as precursor. Al-based MOFs are nontoxic and stable against hydrolysis, which render it an outstanding host material for metal nanoparticles. Upon dispersion of Pd over their surface, the catalysts are characterized by Transmission

^a Shanghai Key Laboratory of Green Chemistry and Chemical Processes, East China Normal University, North Zhongshan Road 3663, 200062 Shanghai, China. E-mail: yjguan@chem.ecnu.edu.cn; Fax: +86 21 32530334

^b Schuit Institute of Catalysis, Department of Chemical Engineering and Chemistry, Eindhoven University of Technology, 5612AZ Eindhoven, The Netherlands

† Electronic supplementary information (ESI) available. See DOI: 10.1039/c3cy00910f

Electron Microscopy (TEM) and X-ray Photo-electron Spectroscopy (XPS). The effect of the organic linker modification on the catalytic activity of supported Pd catalysts is explored and discussed.

Experimental

Materials syntheses

Al-MIL-53-H. The synthesis was carried out under hydrothermal conditions using $\text{Al}(\text{NO}_3)_3 \cdot 9\text{H}_2\text{O}$ and 1,4-benzenedicarboxylic acid (abbreviated as BDC hereafter) in deionized water.²¹ The molar composition of the starting gel was 1 Al (5.20 g):0.5 H_2BDC (1.15 g):80 H_2O , which was placed in a Teflon-lined autoclave for 3 days at 220 °C. The solid product was obtained by filtration.

Al-MIL-53-NH₂. Commercial 2-aminoterephthalic acid ($\text{H}_2\text{BDC-NH}_2$, TCI) was used as the organic linker. Typically, 2.9 g of $\text{AlCl}_3 \cdot 6\text{H}_2\text{O}$ and 2.2 g of $\text{H}_2\text{BDC-NH}_2$ in 30 mL of H_2O were charged in a Teflon-lined autoclave. The autoclave was kept at 150 °C for 5 h. After cooling to room temperature, a yellow precipitate was obtained by filtration.

Al-MIL-53-Cl. 2-Chloroterephthalic acid ($\text{H}_2\text{BDC-Cl}$) was synthesized by oxidation of 2-chloroxylylene with nitric acid.²² In a typical synthesis, 6 ml (43 mmol) of 2-chloroxylylene, 60 mL of deionized water and 16 mL of nitric acid (70%) were charged into a Teflon-lined autoclave. The autoclave was sealed and heated at 170 °C for 16 h (heating rate, 2.5 °C min^{-1}). 2-Chloroterephthalic acid was recovered by filtration as a crystalline white powder, which was further thoroughly washed with hot water and dried under vacuum at 70 °C overnight. The synthesis of Al-MIL-53-Cl was done by a similar hydrothermal synthesis method. A mixture of $\text{AlCl}_3 \cdot 6\text{H}_2\text{O}$ (1.0 g, 4.14 mmol), $\text{H}_2\text{BDC-Cl}$ (0.83 g, 4.14 mmol) and water (40 mL) was charged in a 100 mL Teflon-lined autoclave. The autoclave was heated in an oven at 210 °C for 12 h. The resulting precipitate was obtained by filtration.

Al-MIL-53-OCH₃. 2-Methoxyterephthalic acid ($\text{H}_2\text{BDC-OCH}_3$) was used as the organic linker, which was prepared according to the literature.²³ In a typical synthesis, a mixture of 2,5-dimethylanisole (30 g, 0.22 mol), potassium permanganate (120 g, 0.76 mol) and distilled water (3000 mL) was refluxed for 5 h. The mixture was cooled to room temperature and poured into cold ethanol (2000 mL). This mixture was then filtered, washed thoroughly with water, reduced under vacuum, and acidified with concentrated hydrochloric acid. The resulting white precipitate was collected by filtration, washed with water and vacuum dried. For the synthesis of Al-MIL-53-OCH₃, a mixture of $\text{AlCl}_3 \cdot 6\text{H}_2\text{O}$ (1.0 g, 4.14 mmol), $\text{H}_2\text{BDC-OCH}_3$ (0.75 g, 3.82 mmol), and water (40 mL) was charged in a 100 mL Teflon-lined autoclave, and the autoclave was heated in an oven at 210 °C for 12 h. The white product was obtained by filtration.

Al-MIL-53-NO₂. In a typical synthesis, a mixture of $\text{Al}(\text{NO}_3)_3 \cdot 9\text{H}_2\text{O}$ (1.49 g, 3.97 mmol), $\text{H}_2\text{BDC-NO}_2$ (0.92 g, 4.37 mmol) and water (50 mL) was placed in a 100 mL Teflon-lined autoclave, and the mixture was heated in an

oven at 170 °C for 12 h. After cooling to room temperature, the white microcrystalline product was obtained by filtration.

Activation of Al-MIL-53-X materials

As the thermal stability of product materials with different substituents differs, the activation procedures have been tailored. Pristine Al-MIL-53-H was purified by heating in air at 300 °C for 3 days. Al-MIL-53 modified with OCH_3 , NH_2 , and Cl groups were activated in two steps. 1.0 g of the as-synthesized material was first heated in *N,N*-dimethylformamide (DMF; 2 × 60 mL) at 155 °C for 24 h. The filtered solids were then heated at 155 °C for 24 h. Al-MIL-53-NO₂ (0.5 g) was first heated in methanol (2 × 60 mL) at 80 °C for 48 h and filtered. The white solid was heated at 150 °C for 12 h.

Preparation of Pd catalysts

Supported Pd catalysts were prepared by a deposition–reduction method. Typically, 4.24 mL of H_2PdCl_4 aqueous solution (Pd: 11.8 mg mL^{-1}) was diluted to 40 mL with deionized water. Then 0.95 g of the vacuum dried support was added to the resulting solution and thoroughly stirred for 4 h. The final pH value of the mixture was further adjusted to 9 by adding NaOH solution (1 M). Then, NaBH_4 solution was added to reduce the $\text{Pd}(\text{OH})_2$ under cooling in an ice bath with vigorous stirring.¹¹ The catalysts were filtered and dried at 90 °C under vacuum overnight. The vacuum-dried catalysts were cooled to room temperature. Before being taken out of the oven, the vacuum valve was released slowly allowing for slow exposure to air, which avoided undesired combustion.

Characterization of Al-MIL-53-X and Pd/Al-MIL-53-X

Powder X-ray diffraction (XRD) patterns were collected using a Rigaku Ultima IV X-ray diffractometer with Cu K α radiation ($\lambda = 1.5405 \text{ \AA}$) operated at 35 kV and 25 mA. Scanning electron microscopy (SEM) was performed using a Hitachi S-4800 microscope. Transmission electron microscopy (TEM) images were taken using a FEI Tecnai G2 F30 microscope operating at 300 kV. The average Pd particle size was calculated using $d_{\text{TEM}} = (\sum n_i d_i^3) / (\sum n_i d_i^2)$ by measuring at least 100 particles. The Pd loading was determined using a Thermo Elemental IRIS Intrepid II XSP inductively coupled plasma emission spectrometer (ICP-AES). The desired amount of sample was dissolved in 10 mL of *aqua regia*. The solution was heated to remove the residual acid and diluted in a 50 mL volumetric flask. Pulse CO chemisorption was performed using a Micromeritics AutoChem 2910 to determine the metal dispersion of the reduced catalysts. Prior to the measurement, an amount of 100 mg catalyst was reduced in a flow of 80 mL min^{-1} of 10 vol.% H_2 in Ar at 150 °C for 3 h and then flushed in He for 1 h. After cooling to 35 °C in He, the CO gas pulses (5 vol.% in He) were introduced in a flow of 80 mL min^{-1} . The changes in the CO gas phase concentration were followed by TCD. CO pulsing was repeated until the pulse area did not change anymore. XPS spectra of fresh Pd catalysts were recorded using a Kratos AXIS Ultra DLD spectrometer with a

monochromated Al K α radiation source. The survey spectra were recorded with a pass energy of 160 eV and the high-resolution spectra with a pass energy of 40 eV to identify the chemical state of each element. All the binding energies (BEs) were referenced to the C 1s neutral carbon peak at 284.6 eV.

Phenol adsorption

The phenol adsorption behaviors on substituted Al-MIL-X were performed as described elsewhere.¹¹ Typically, 50 mg of the dried sample was used for the adsorption in phenol solutions with various initial phenol concentrations (0.05, 0.1, 0.15, 0.2, and 0.25 M) at 20 °C. Before adsorption, MIL-X was dried under vacuum at 140 °C for 2 h. The dried powder (50 mg) was added to the aqueous phenol solutions (50 mL) and vigorously stirred for 6 h. After adsorption, the solution was recovered by centrifugation and diluted, and the equilibrium phenol concentration was determined using the absorbance at 270 nm using a Shimadzu UV-2550 ultraviolet visible spectrophotometer. The calibration curve was obtained from the UV spectra of standard solutions (10–125 μ M).

Catalytic reaction tests

Phenol hydrogenation. A Teflon-lined (120 mL) batch reactor was used to carry out the liquid phase hydrogenation. No specific pretreatment was conducted prior to the reaction. An amount of 100 mg of the catalyst was mixed with 10 mL of aqueous phenol solution (0.25 M) into a Teflon-lined steel batch reactor. The reactor was purged five times with H₂ and then pressurized with 5 bar H₂. The reaction was conducted at 20, 35, 50, and 90 °C and kept for 24, 6, 5, and 2 h, respectively. The products were analysed using a Shimadzu GC 2014 equipped with a DB-Wax capillary column (30 m length and 0.25 mm internal diameter). The main product was cyclohexanone with cyclohexanol as the only by-product.

Phenylacetylene hydrogenation. The hydrogenation of phenylacetylene was performed in a 50 mL three-neck flask at 40 °C under atmospheric pressure. In a typical experiment, 9.1 mmol phenylacetylene and 10 mg of catalyst was mixed with 9 mL of methanol. 20 mL min⁻¹ of H₂ was continuously bubbled through the liquid phase with vigorous stirring. Samples were withdrawn at the desired period, diluted with methanol, and analysed using GC.

Results and discussion

Characterization of Al-MIL-53 structures

All Al-MIL-53 structures were activated and purified thoroughly before use as supports. A previous study has shown that the unreacted terephthalic acid gives an IR band in the region 1694–1711 cm⁻¹ assigned to its protonated form (-CO₂H), whereas DMF shows a strong absorption band in the range 1663–1673 cm⁻¹ due to the carbonyl stretching vibration.²¹ The absence of these bands in the IR spectra (Fig. 1) suggests the complete removal of solvents and residual terephthalic acid in the activation steps. XRD patterns of the activated samples are

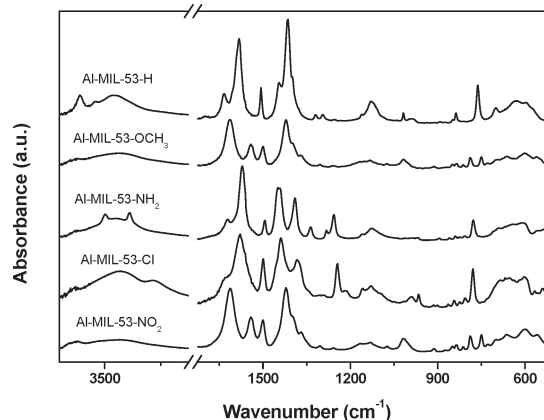


Fig. 1 IR spectra of activated Al-MIL-53-X (X = H, OCH₃, NH₂, Cl, and NO₂) materials.

shown in Fig. 2 and clearly confirm that all materials had the MIL-53 structure.²¹ The BET surface areas of Al-MIL-53-X (X = H, OCH₃, NH₂, Cl, and NO₂) are 1728, 182, 113, 187, and 82 m² g⁻¹, respectively, calculated from their N₂ adsorption isotherm curves (see Fig. S1†). Introducing organic groups resulted in a significant decrease of the surface area, partially due to the blockage of micropores and/or pore collapse during the pre-treatment.

Unlike Cr-based MOFs, Al-based MIL-53 has been considered to be an environmentally friendly and highly promising candidate for industrial applications.²⁴ It has been reported to be a promising support of Pd catalysts for such organic reactions as Heck and Suzuki-Miyaura cross-coupling reactions.^{25,26} The structure of MIL-53 is hydrophobic, therefore limiting the wetting of its pores by the aqueous solution of palladium chloride.¹¹ We have roughly estimated the hydrophobicity of Al-MIL-53-X by conducting TG analysis (Fig. 3). Two weight losses are clearly observed for all materials. The first weight loss at temperature below 100 °C is due to water desorption, showing that Al-MIL-5-X materials are relatively hydrophilic. From the weight loss percentage we can conclude

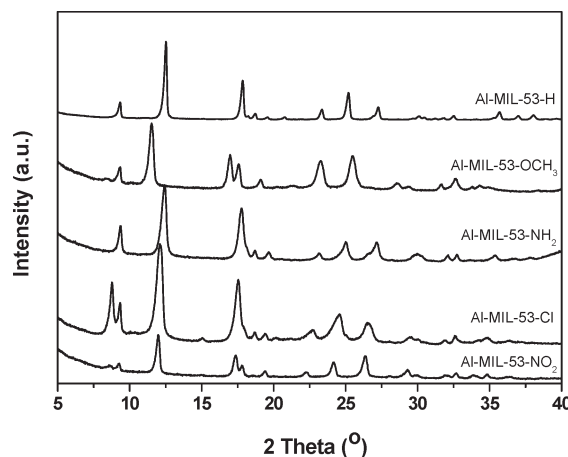


Fig. 2 XRD profiles of Al-MIL-53-X (X = H, OCH₃, NH₂, Cl, and NO₂) catalysts.

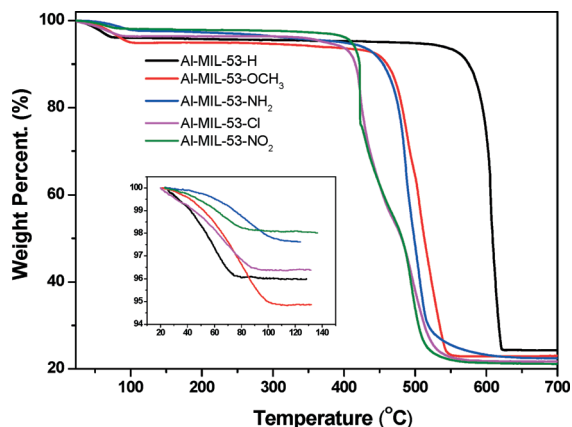


Fig. 3 TG curves of the activated Al-MIL-53-X (X = H, OCH₃, NH₂, Cl, and NO₂) materials in N₂ with a ramp rate of 10 °C min⁻¹. (The inset is the TG curves in the range of 20 to 130 °C).

that the organic substituents indeed change the hydrophobicity of Al-MIL-53. Lower weight loss due to water desorption on NH₂-, Cl-, and NO₂-modified MIL-53 points to their lower hydrophilicity consistent with a previous report.²¹ In comparison, -OCH₃ results in higher hydrophilicity, probably due to stronger H-bonding between water molecules and the methoxy groups. Another observation obtained from TG analysis is that these Al-MIL-53-X materials display different thermal stabilities following the trend of -H (600 °C) > -NH₂ ≈ -OCH₃ (500 °C) > -Cl ≈ -NO₂ (400 °C). The lower thermal stability of Al-MIL-53-X with substituent groups is attributed to the dissociation of the C-X bond of these functional groups.

Characterization of Pd/MIL-53 catalysts

No X-ray diffraction of palladium (not shown) was observed for the Pd/MIL-53-X catalysts, probably due to the relatively low loading, which was about 3 wt.% (Table 1). We measured the BET surface areas of two supported Pd catalysts, namely Pd/Al-MIL-53-H and Pd/Al-MIL-53-NO₂, to be 1011 and 98 m² g⁻¹ calculated from N₂ adsorption isotherms (Fig. S2[†]), respectively. The BET area of Pd/Al-MIL-53-H is rather lower than that of the pristine material, whereas a similar BET area is observed for Pd/Al-MIL-53-NO₂ and the corresponding support. This result suggests that the Pd nanoparticles are not embedded in the pores but are mainly located on the external surface.

The particle size distribution of the active Pd phase was determined by high-resolution TEM (Fig. 4). The Pd

nanoparticles in Pd/Al-MIL-53-H had sizes in the range of 2–5 nm with an average size of 4.3 ± 1.0 nm. By introducing OCH₃, NH₂, Cl, NO₂ groups, the average particle size changed to 2.4 ± 0.45 nm, 3.8 ± 1.0 nm, 3.4 ± 0.77 nm, and 2.4 ± 0.53 nm, respectively. Thus, the substituents clearly improve the dispersion of Pd nanoparticles consistent with previous reports.^{25–27} The total accessible metal surface area was estimated by pulse CO chemisorption measurements. The dispersion of Pd on Al-MIL-53-H, -OCH₃, -NH₂, -Cl, and -NO₂ was 32%, 33%, 40%, 14% and 24%, respectively. The average particle size calculated based on the dispersion was 3.4, 3.3, 2.8, 7.5 and 4.6 nm, respectively. These values show distinct differences from the values obtained by HRTEM analyses. For H and NH₂ groups, similar Pd particle sizes were observed, whereas a much larger particle size was found from CO chemisorption for Cl- and NO₂-modified Al-MIL-53. We should like to note that the electron withdrawing groups may inhibit CO chemisorption on Pd to some extent.

The fresh catalysts were characterized by XPS (Fig. 5), which was used to establish the oxidation state of Pd under ambient conditions. The doublet Pd 3d_{5/2} peaks at 335.3 and 337.3 eV are clearly observed for all catalysts and are assigned to metallic Pd and oxidized Pd species, respectively.^{25,28–30} This result evidences the presence of both Pd²⁺ and Pd⁰ in the nanoparticles. The Pd²⁺/Pd⁰ ratios obtained from the deconvolution of the Pd 3d region spectra are summarized in Table 1. It can be seen that Pd⁰ is the dominating species on MIL-53-H. Introducing substituent groups significantly increased the amount of Pd²⁺ species of palladium catalysts. The proportion of Pd²⁺ increases following the trend of H < OCH₃ < NH₂ < Cl < NO₂. It is well known that Pd nanoparticles can be easily reoxidized upon exposure to air. Moreover, the smaller the particle size, the more easily Pd is oxidized. Obviously, these results confirm our speculation that the reason for the deviation between CO chemisorption and TEM results may be incomplete reduction of Pd or changes in its electronic nature when interacting with the modified MOF surface. The trend is consistent with TEM, evidencing that very small Pd particles were formed on the modified Al-MIL-53-X.

The reducibility of these Pd nanoparticles was characterized by H₂-TPR and the results are shown in Fig. S3.[†] Oxidic Pd^{δ+} was reduced readily at room temperature for all catalysts, meaning that Pd nanoparticles were mainly in the metallic state in the hydrogenation process. Upon exposure to H₂, Pd hydrides with various H/Pd ratios were formed depending on

Table 1 Loading, particle sizes and oxidation states of supported Pd catalysts

Pd/Al-MIL-53-X	Loading (wt.%)	<i>d</i> _{TEM} (nm)	Dispersion ^a (%)	Pd ⁰		Pd ²⁺	
				BE (eV)	Ratio (%)	BE (eV)	Ratio (%)
H	2.8	4.3	32	335.4	70.0	337.2	30.0
OCH ₃	3	2.4	33	335.9	63.4	337.4	36.6
NH ₂	3	3.8	40	335.7	62.8	337.5	37.2
Cl	2.9	3.4	14	335.5	54.5	337.5	45.5
NO ₂	3	2.4	24	335.6	45.0	337.6	55.0

^a Based on the total Pd loading and CO chemisorption amount. An assumption of CO/Pd⁰ = 1 was used.

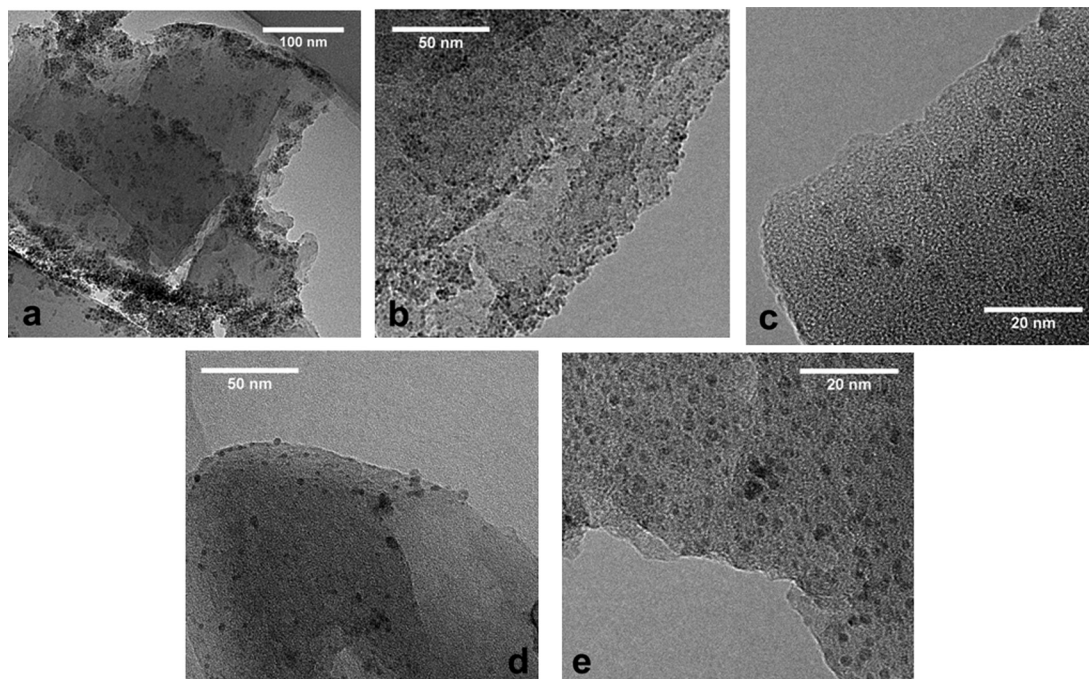


Fig. 4 TEM images of Pd nanoparticles supported on a) Al-MIL-53-H, b) Al-MIL-53-OCH₃, c) Al-MIL-53-NH₂, d) Al-MIL-53-Cl, and e) Al-MIL-53-NO₂.

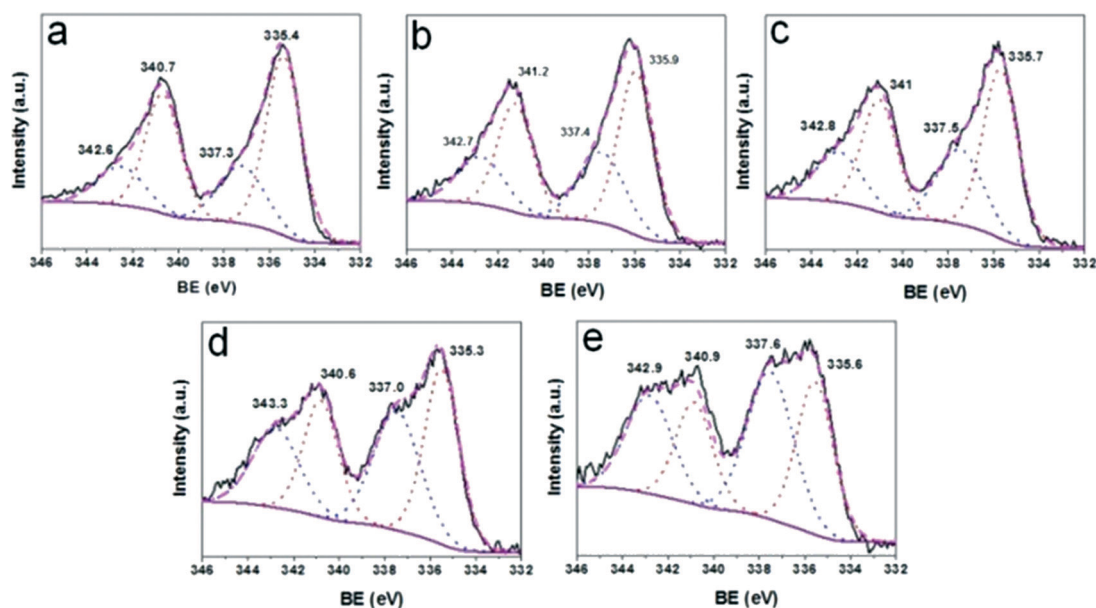


Fig. 5 XPS spectra of Pd nanoparticles supported on a) Al-MIL-53-H, b) Al-MIL-53-OCH₃, c) Al-MIL-53-NH₂, d) Al-MIL-53-Cl, and e) Al-MIL-53-NO₂.

the electronic properties of the modified groups. Higher values of H/Pd ratios on electron withdrawing groups (0.18 and 0.22 for Cl and NO₂, respectively) than the values on electron donating groups (0.03 and 0.05 for NH₂ and OCH₃, respectively) were observed. The H/Pd ratio on the unmodified Pd/MIL-53 was about 0.11. It is generally accepted that the H/Pd ratio is related to the Pd particle size, with a higher value on bigger particles (*ca.* 0.67 maximum) and with smaller particles (<2.5 nm) showing negligible Pd hydride formation.³¹ The catalytic role of these Pd hydrides on Pd/C catalysts in liquid phase hydrogenation

has been emphasized recently by an *in situ* XAFS study, which was not perturbed by water and reaction intermediates.³²

Catalytic activity tests

Selective hydrogenation of phenol. Considering the industrial importance of selective hydrogenation of phenol to cyclohexanone, we tested the catalytic activity of Pd/MIL-Xs in this reaction. The reactions were carried out in a Teflon-lined steel autoclave under 0.5 MPa H₂ with a phenol/Pd ratio

of 83. We first investigated the effect of the reaction temperature on the hydrogenation activity of Pd-Al-MIL-X, *i.e.*, 19, 35, and 50 °C. The results including phenol conversion and cyclohexanone selectivity are collected in Table 2. All Pd catalysts were active for phenol hydrogenation at 19 °C. The phenol conversions after reaction for 24 h for various catalysts were in the range of 8.4 to 36.3%, with selectivity to cyclohexanone above 95% in all cases. We compared the activity of the 5 wt.% Pd/Al₂O₃ catalyst (from Alfa-Aesar); 27.0% of phenol conversion was observed after reaction for 24 h using 50 mg of the catalyst (phenol/Pd ratio of 100) and at 25 °C under otherwise similar conditions, with a lower cyclohexanone selectivity of 79.3%. This result further evidences the advantage of MOFs as the support of Pd nanoparticles for hydrogenation under mild conditions.^{12,13}

The conversion follows the trend of H (36.3%) > OCH₃ (30.4%) > NH₂ (25%) > Cl (11.5%) > NO₂ (8.4%). The turnover frequencies (TOFs) are calculated to be 1.5, 1.1, 0.94, 0.45, and 0.3 h⁻¹ for H-, OCH₃-, NH₂-, Cl- and NO₂-modified Al-MIL-53 with the corresponding conversions, respectively. Amongst all Pd catalysts studied, the pristine MIL-53 supported Pd catalyst showed the highest catalytic activity. When the reaction temperature increased up to 35 °C, the reaction time was shortened four times to 6 h. The turnover frequencies are calculated to be 5.4, 4.9, 5.1, 2.2, and 2.0 h⁻¹ for H-, OCH₃-, NH₂-, Cl- and NO₂-modified Pd catalysts, respectively. Under these reaction conditions, the reactivities of OCH₃ and NH₂ substituted MIL-53s were the same as that of the pristine material, whereas Cl- and NO₂-functionalized materials showed a significantly lower activity. With the temperature further increased to 50 °C, we found that the TOF increased to 15.2, 16.5, 16.3, 8.9 and 9.5 h⁻¹ for H-, OCH₃-, NH₂-, Cl- and NO₂-modified Pd catalysts, respectively. At 50 °C, the commercial 5 wt.% Pd/Al₂O₃ catalyst gave a phenol conversion of 76.5% and cyclohexanone selectivity of 98.4% after reaction for 4 h.

Table 2 Catalytic performance of Pd/Al-MIL-53-X catalysts for phenol selective hydrogenation^a

Pd/Al-MIL-53-X	T/°C	X _{phenol} /%	Sel./%		TOF/h ⁻¹	E _a /kJ mol ⁻¹
			C=O	C-OH		
H	19 (24)	36.3	97.2	2.8	1.5	59
	35 (6)	33.9	98.2	1.6	5.4	
	50 (5)	79.0	96.6	3.4	15.2	
OCH ₃	19 (24)	30.4	94.1	5.9	1.1	68
	35 (6)	38.5	95.8	4.2	4.9	
	50 (5)	91.8	94.2	5.8	16.5	
NH ₂	19 (24)	25.0	95.0	5.0	0.94	72
	35 (6)	33.9	97.9	2.1	5.1	
	50 (5)	90.6	97.0	3.0	16.3	
Cl	19 (24)	11.5	97.4	2.6	0.45	76
	35 (6)	14.3	98.6	1.4	2.2	
	50 (5)	48.0	96.4	3.6	8.9	
NO ₂	19 (24)	8.4	95.2	4.8	0.3	86
	35 (6)	13.2	96.2	3.8	2.0	
	50 (5)	53.0	96.2	3.8	9.5	

^a Reaction conditions: 100 mg catalyst, 10 ml 0.25 M aqueous phenol solution, 0.5 MPa H₂.

Based on the TOFs at different temperatures, we calculated the apparent activation energy (E_{act}) for the Pd catalysts in the selective hydrogenation of phenol (Fig. 6), and the results are listed in Table 2. The E_{act} is in the range of 59–86 kJ mol⁻¹. These values are in good agreement with previous reports suggesting that the reaction rate is not limited by mass transfer.^{33,34} The activation energy and reactivity show a clear opposite trend, with Pd/MIL-53 displaying the lowest activation energy of 59 kJ mol⁻¹ and having the highest activity. On the other hand, the surface hydrophilicity and/or hydrophobicity may also contribute to the E_a of the hydrogenation reaction. Wang *et al.*³⁵ proposed a water promoted H₂ activation mechanism with a very low E_a of 35.9 kJ mol⁻¹ inspired by the H₂-D₂O exchange during hydrogenation process, which explained well the superior catalytic activity of Pd catalysts in aqueous phase than in organic solvents for hydrogenation. In this regard, catalysts with higher hydrophilicity allowing for easier accessibility of H₂O will give lower E_a values, as is observed in this study. Much lower activation energies are found on the unmodified catalyst, therefore enhancing the hydrogenation activity.

At 90 °C these Pd catalysts showed very similar catalytic activities (Table 3). It is likely that modified MOFs perform better at higher temperatures. This might therefore represent a case of enthalpy-entropy compensation.

Previous studies have shown that high phenol adsorption capacity on the support is needed to ensure high catalytic activity and selectivity to cyclohexanone, as observed on polyaniline-functionalized carbon-nanotubes, MOFs and mpg-C₃N₄.^{8,11,35} It has been assumed that phenol adsorbed in a nonplanar fashion gives rise to cyclohexanone.^{8,35} In this study, the phenol adsorption capacities of Al-MIL-53-X have also been

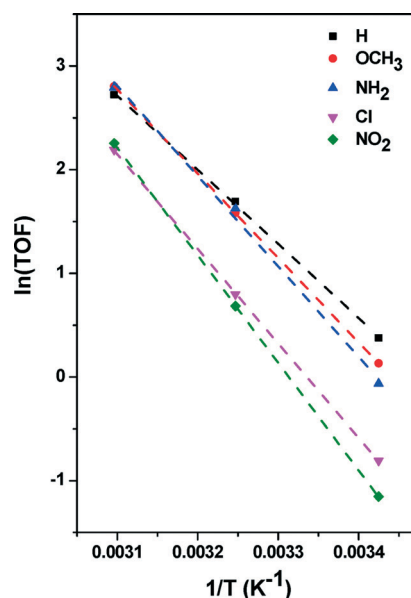


Fig. 6 Arrhenius plots for the hydrogenation of phenol on 3 wt.% Pd/Al-MIL-53-X (X = H, OCH₃, NH₂, Cl, and NO₂) catalysts in the temperature range of 20–50 °C (100 mg catalyst, 10 ml of 0.25 M aqueous phenol solution, and 0.5 MPa H₂).

compared. The pristine Al-MIL-53-H material showed the highest phenol adsorption capacity (Fig. 7). Introducing organic linkers remarkably decreased the phenol adsorption capacities due to the significant loss of surface area. However, the decrease of phenol uptake is not linear to the loss of surface area, meaning that a strong interaction occurs between phenol and the framework of MIL-53. Similar values on modified Al-MIL-53 materials were obtained regardless of the linkers. Given the similar phenol adsorption behavior on Al-MIL-53-X with mono-substituent, it is safe to conclude that the activity of Pd/Al-MIL-53s is more likely related to the electronic properties of the framework linkers rather than the adsorption ability of phenol on different materials.

Phenylacetylene hydrogenation. The reactivity of these Pd nanoparticles in semi-hydrogenation using phenylacetylene as a substrate instead of phenol was conducted and the results are shown in Table 4. This reaction has been widely applied to characterize the catalytic activity of supported Pd catalysts.³⁶ Under the tested reaction conditions, H-, OCH₃-, and NH₂-functionalized Pd catalysts again showed much better catalytic activity than Cl- and NO₂-modified Pd catalysts. Amino functionalized Pd/MIL-53 showed the best catalytic activity, giving 24.7% conversion of phenylacetylene and 98.8% selectivity to styrene after 0.5 h. The TOF is close to that reported on cross-linked ionic liquid polymer supported Pd catalysts.³⁷ Extending the reaction time to 2 h led to nearly total conversion (>99.9%) of phenylacetylene and selectivity of 78.0% to styrene. The electron donating group-modified Pd/Al-MIL-53 catalysts showed higher catalytic activity than conventional inorganic oxide-supported Pd catalysts.³⁶ Due to the lower hydrogen

Table 4 Semihydrogenation of phenylacetylene on Pd supported on Al-MIL-53s with various organic linkers

Pd/Al-MIL-53-X	<i>t</i> = 0.5 h		<i>t</i> = 2 h		TOF ^c (s ⁻¹)
	<i>X</i> ^a	<i>S</i> ^b	<i>X</i>	<i>S</i>	
H	19.5	99	>99.9	94.5	0.35
OCH ₃	18.0	98.0	80.0	96.0	0.32
NH ₂	24.7	98.8	>99.9	78.0	0.44
Cl	13.3	98.5	46.9	97.0	0.24
NO ₂	9.4	93.6	34.5	93.3	0.17

Reaction conditions: 10 mg catalyst, 1 ml phenylacetylene dissolved in 10 ml of methanol, 43 °C, 1 bar H₂ with a flow rate of 20 mL min⁻¹.^a Conversion of phenylacetylene. ^b Selectivity to styrene. ^c Calculated by Pd loading.

activation and transfer activity of electron withdrawing linkers, Pd/Al-MIL-53-Cl (NO₂) showed a rather lower hydrogenation activity. These results further point to the effect of organic linkers in hydrogen activation on Pd nanoparticles.

The utilization of a stable and environmentally benign Al-based MOF as a support material for hydrogenation catalysts would be interesting for future industrial applications. The results presented in this study demonstrate that Pd nanoparticles supported on Al-MIL-53 exhibit excellent catalytic performance in selective hydrogenation reactions. Organic substituent groups remarkably affect the catalytic activities of supported Pd nanoparticles. Electron-donating group (NH₂- and OCH₃-) modified catalysts show much higher activity than their electron-withdrawing (Cl- and NO₂-) counterparts. It should be noted that NH₂- and OCH₃-functionalized materials showed a much lower surface area than the unmodified counterpart but a similar catalytic activity was achieved, thereby emphasizing the importance of the electronic structure of supports in governing the catalytic activity of supported Pd nanoparticles.³⁸

Conclusions

In summary, the catalytic hydrogenation activity of 3 wt.% Pd/Al-MIL-53-X catalysts with various organic linkers (X = H, OCH₃, NH₂, Cl, and NO₂) has been systematically studied. The surface of Al-MIL-53-H is relatively hydrophilic and has a very high surface area (1728 m² g⁻¹), which benefit the support of Pd nanoparticles. Al-MIL-53-X with organic linkers containing NH₂, Cl, and NO₂ are more hydrophobic and show a much lower surface area (varying from 82 to 187 m² g⁻¹). Despite the hydrophobic nature and lower surface area of modified Al-MIL-53-X, Pd nanoparticles with very similar and narrow distribution in the range of 2–5 nm were successfully supported favored by the interaction between Pd and organic linkers. Fresh Pd nanoparticles mainly existed as a mixture of Pd(II) and Pd(0) when exposed to air, but easily became metallic upon reduction at room temperature. Compared with electron donating groups (H, NH₂, and OCH₃), electron withdrawing groups (Cl and NO₂) might inhibit the CO adsorption on the Pd surface, as well as hydrogen dissociation. Pd/Al-MIL-53-X showed distinctly different catalytic hydrogenation activities at room

Table 3 Catalytic performance of Pd/Al-MIL-53-X catalysts for phenol selective hydrogenation at 90 °C^a

Pd/Al-MIL-53-X	Conv. (%)	TOF (h ⁻¹)	Sel. (%)	
			C=O	-OH
H	97.5	46	94.8	5.2
OCH ₃	99.4	44	81.9	18.1
NH ₂	98.8	44	95.1	4.9
Cl	97	45	96.2	3.8
NO ₂	99.1	44	87.7	12.3

^a Reaction conditions: 100 mg of catalyst, 10 ml of 0.25 M aqueous phenol solution, 0.5 MPa H₂, 90 °C, reaction for 2 h.

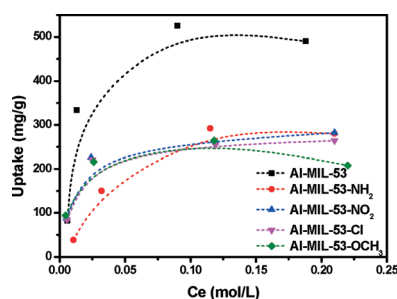


Fig. 7 Phenol adsorption capacities (mg_{phenol} g_{MIL-53}⁻¹) on Al-MIL-53 with various organic linkers under different equilibrium concentrations.

temperature and 0.5 MPa H₂, with turnover frequencies of 1.5, 1.1, 0.94, 0.45, and 0.3 h⁻¹ for H-, OCH₃-, NH₂-, Cl- and NO₂-modified Pd/Al-MIL-53 catalysts, respectively. The modification by electron withdrawing groups led to activation energies of 76 and 86 kJ mol⁻¹ for Pd/Al-MIL-53-Cl and -NO₂, respectively, much higher than that for the pristine Pd/Al-MIL-53-H (59 kJ mol⁻¹). This might be attributed to two effects: the interaction between Pd and organic linkers and the surface hydrophobicity brought by the linkers.

Acknowledgements

We acknowledge the financial support from the National Natural Science Foundation of China (grant no. 21203065) and the Fundamental Research Funds for the Central Universities.

Notes and references

- 1 A. Balanta, C. Godard and C. Claver, *Chem. Soc. Rev.*, 2011, **40**, 4973.
- 2 I. P. Beletskaya and A. V. Cheprakov, *Chem. Rev.*, 2000, **100**, 3009.
- 3 C. O. Bennett and M. Che, *J. Catal.*, 1989, **120**, 293.
- 4 P. Kacer and L. Cerveny, *Appl. Catal., A*, 2002, **229**, 193.
- 5 H. Liu, T. Jiang, B. Han, S. Liang and Y. Zhou, *Science*, 2009, **326**, 1250.
- 6 S. Vyver and Y. Roman-Leshkov, *Catal. Sci. Technol.*, 2013, **3**, 1465.
- 7 Y. Wang, J. Yao, H. Li, D. Su and M. Antonietti, *J. Am. Chem. Soc.*, 2011, **133**, 2362.
- 8 J. Chen, W. Zhang, L. Chen, L. Ma, H. Gao and T. Wang, *ChemPlusChem*, 2013, **78**, 142.
- 9 A. Chen, G. Zhao, J. Chen, L. Chen and Y. Yu, *RSC Adv.*, 2013, **3**, 4171.
- 10 H. Liu, Y. Li, R. Luque and H. Jiang, *Adv. Synth. Catal.*, 2011, **353**, 3107.
- 11 D. Zhang, Y. Guan, E. J. M. Hensen, L. Chen and Y. Wang, *Catal. Commun.*, 2013, **41**, 47.
- 12 A. Dhakshinamoorthy and H. Garcia, *Chem. Soc. Rev.*, 2012, **41**, 5262.
- 13 J. Juan-Alcaniz, J. Gascon and F. Kapteijn, *J. Mater. Chem.*, 2012, **22**, 10102.
- 14 S. Opelt, S. Turk, E. Dietzsch, A. Henschel, S. Kaskel and E. Klemm, *Catal. Commun.*, 2008, **9**, 1286.
- 15 P. Wang, J. Zhao, X. Li, Y. Yang, Q. Yang and C. Li, *Chem. Commun.*, 2013, **49**, 3330.
- 16 B. Yuan, Y. Pan, Y. Li, B. Yin and H. Jiang, *Angew. Chem., Int. Ed.*, 2010, **49**, 4054.
- 17 T. Ishida, M. Nagaoka, T. Akita and M. Haruta, *Chem.-Eur. J.*, 2008, **14**, 8456.
- 18 H. Pan, X. Li, D. Zhang, Y. Guan and P. Wu, *J. Mol. Catal. A: Chem.*, 2013, **377**, 108.
- 19 E. Chen, Y. Liu, T. Sun, Q. Wang and L. Liang, *Chem. Eng. Sci.*, 2013, **97**, 60.
- 20 F. Vermoortele, M. Vandichel, B. Voorde, R. Ameloot, M. Waroquier, V. Speybroeck and D. E. De Vos, *Angew. Chem., Int. Ed.*, 2012, **51**, 4887.
- 21 S. Biswas, T. Ahnfeldt and N. Stock, *Inorg. Chem.*, 2011, **50**, 9518.
- 22 T. Devic, P. Horcajada, C. Serre, F. Salles, G. Maurin, B. Moulin, D. Heurtaux, G. Clet, A. Vimont, J. M. Greneche, B. L. Ouay, F. Moreau, E. Magnier, Y. Filinchuk, J. Marrot, J. C. Lavalley, M. Daturi and G. Ferey, *J. Am. Chem. Soc.*, 2010, **132**, 1127.
- 23 Y. Chen, R. Wombacher, J. H. Wendorff and A. Greiner, *Polymer*, 2003, **44**, 5513.
- 24 M. Gaab, N. Trukhan, S. Maurer, R. Gummaraju and U. Muller, *Microporous Mesoporous Mater.*, 2012, **157**, 131.
- 25 Y. Huang, S. Gao, T. Liu, J. Lu, X. Lin, H. Li and R. Cao, *ChemPlusChem*, 2012, **77**, 106.
- 26 M. A. Gotthardt, A. Beilmann, R. Schoch, J. Engelke and W. Kleist, *RSC Adv.*, 2013, **3**, 10676.
- 27 Y. Huang, Z. Zheng, T. Liu, J. Lv, Z. Lin, H. Li and R. Cao, *Catal. Commun.*, 2011, **14**, 27.
- 28 C. Evangelisti, N. Panziera, P. Pertici, G. Vitulli, P. Salvadori, C. Battocchio and G. Polzonetti, *J. Catal.*, 2009, **262**, 287.
- 29 Y. Shao, Z. Xu, H. Wan, Y. Wan, H. Chen, S. Zheng and D. Zhu, *Catal. Commun.*, 2011, **12**, 1405.
- 30 J. A. Baeza, L. Calvo, M. A. Gilarranz, A. F. Mohedano, J. A. Casas and J. J. Rodriguez, *J. Catal.*, 2012, **293**, 85.
- 31 C. Zlotea, F. Cuevas, V. Paul-Boncour, E. Leroy, P. Dibandjo, R. Gadiou, C. Vix-Guterl and M. Latroche, *J. Am. Chem. Soc.*, 2010, **132**, 7720.
- 32 Z. A. Chase, J. L. Fulton, D. M. Camaioni, D. H. Mei, M. Balasubramanian, V.-T. Pham, C. Zhao, R. S. Weber, Y. Wang and J. A. Lercher, *J. Phys. Chem. C*, 2013, **117**, 17603.
- 33 J. R. Gonzalez-Velasco, M. P. Gonzalez-Marcos, S. Arnaiz, J. I. Gutierrez-Ortiz and M. A. Gutierrez-Ortiz, *Ind. Eng. Chem. Res.*, 1995, **34**, 1031.
- 34 N. Mahata and V. Vishwanathan, *J. Catal.*, 2000, **196**, 262.
- 35 Y. Li, X. Xu, P. Zhang, Y. Gong, H. Li and Y. Wang, *RSC Adv.*, 2013, **3**, 10973.
- 36 S. Dominguez-Dominguez, A. Berenguer-Murcia, A. Linares-Solano and D. Cazorla-Amoros, *J. Catal.*, 2008, **257**, 87.
- 37 Y. Zhang, X.-Y. Quek, L. Wu, Y. Guan and E. J. M. Hensen, *J. Mol. Catal. A: Chem.*, 2013, **379**, 53.
- 38 P. Chen, L. M. Chew, A. Kostka, M. Muhler and W. Xia, *Catal. Sci. Technol.*, 2013, **3**, 1964.